



STRUCTURAL SCIENCE
CRYSTAL ENGINEERING
MATERIALS

Volume 80 (2024)

Supporting information for article:

**ELASTIC AND PIEZOELECTRIC PROPERTIES OF β -GLYCINE - A
QUANTUM CRYSTALLOGRAPHY VIEW ON INTERMOLECULAR
INTERACTIONS AND A HIGH-PRESSURE PHASE TRANSITION**

Mark Khainovsky, Elena Boldyreva and Vladimir Tsirelson

Table S1 Unit cell parameters and volume of β - (space group $P2_1$) and β' -glycine (space group $P2_1/c$) calculated at various external pressures*

Pressure, GPa	a, Å	b, Å	c, Å	β , grad	V, Å ³
Low Pressure Phase (β -glycine)					
0	5.357	5.954	4.992	113.23	146.04
	5.378	6.174	5.065	111.87	156.07
	5.388(2)	6.276(2)	5.091(2)	113.12(3)	158.31(10)
	5.388(1)	6.130(3)	5.067(1)	113.52(1)	153.39(12)
0.2	5.354	5.932	4.983	113.50	145.14
	5.375	6.143	5.056	112.06	154.69
	5.381(1)	6.217(2)	5.076(2)	113.42(2)	155.81(10)
0.4	5.351	5.911	4.975	113.66	144.12
	5.372	6.114	5.046	112.25	153.38
	5.378(1)	6.184(2)	5.062(1)	113.64(2)	154.22(10)
0.7	5.346	5.882	4.963	113.91	142.67
	5.367	6.072	5.032	112.52	151.51
	5.375(8)	6.125(1)	5.051(1)	113.93(1)	151.80(10)
High pressure phase (β' -glycine)					
0.9	5.329	5.843	9.870	113.98	280.80
	5.364	6.113	9.936	112.92	300.09
	5.367(3)	6.010(3)	10.010(3)	114.16(6)	294.60(10)
1.7	5.31	5.764	9.836	114.31	274.36
	5.346	5.974	9.906	113.47	290.21
	5.363(4)	5.932(3)	9.979(2)	114.33(6)	289.27(10)

* The experimental variable-pressure data at ambient temperature were taken from Tumanov *et al.* (2008). The first line corresponds to calculations with D3 dispersion correction (red), the second line reports results without dispersion correction D3 (blue), and the third line represents experimental XRD data (green). The fourth line at 0 GPa (black) corresponds to single-crystal variable-temperature data from Boldyreva *et al.*, (2003) extrapolated to 0 K.

Table S2 Calculated characteristics of covalent bonds at different pressures

Pressure, GPa	0	0	0.2	0.4	0.7	0.9	1.7
	experimental						
	Bond length, Å						

C1-C2	1.616(10)	1.523	1.522	1.521	1.521	1.521	1.519
C1-O1	1.224(20)	1.256	1.256	1.256	1.256	1.256	1.256
C1-O2	1.241(10)	1.261	1.261	1.261	1.261	1.260	1.261
C2-N1	1.498(20)	1.471	1.471	1.469	1.468	1.469	1.467
Angle, degree							
O1-C1-O2	126(2)	126	126	126	125	125	125
O1-C1-C2	117(1)	117	117	118	118	117	118
O2-C1-C2	117(1)	117	117	117	117	117	118
C1-C2-N1	112(1)	113	112	112	112	112	112

Table S3 Topological characteristics at the hydrogen bonds critical points (BCPs) in β - and β' -glycine.

P, GPa	Bond type	$r_{(O...H)}$, Å	Electron density ρ , a.u.	Laplacian of electron density, $\nabla^2\rho$, a.u.	Virial energy density, v , a.u.	Kinetic energy density, g , a.u.	E_{H-bond} , kJ/mol (Vener <i>et al.</i> , 2012)	QEP, a.u. (Tsirelson <i>et al.</i> , 2016)	Ellipticity of H-bonds, ϵ
Low pressure phase (β -glycine)									
0	I	1.774	0.0381	0.109	-0.028	0.028	36.50	-0.0119	0.021
	II	1.664	0.0518	0.137	-0.040	0.037	48.84	-0.0094	0.022
	III	2.233	0.0134	0.047	-0.015	0.011	14.70	-0.0043	0.070
	IV	2.118	0.0190	0.058	-0.011	0.015	19.17	-0.0046	0.095
0.2	I	1.769	0.0386	0.111	-0.029	0.028	37.02	-0.0090	0.022
	II	1.662	0.0521	0.137	-0.041	0.037	49.10	-0.0095	0.023
	III	2.230	0.0135	0.048	-0.018	0.011	14.84	-0.0044	0.075
	IV	2.104	0.0196	0.059	-0.015	0.015	19.82	-0.0047	0.092
0.4	I	1.765	0.0390	0.112	-0.029	0.029	37.42	-0.0091	0.022
	II	1.660	0.0523	0.138	-0.041	0.038	49.36	-0.0094	0.028
	III	2.227	0.0136	0.048	-0.011	0.011	14.97	-0.0044	0.079
	IV	2.091	0.0201	0.060	-0.016	0.016	20.35	-0.0048	0.090

0.7	I	1.758	0.0397	0.114	-0.030	0.029	38.20	-0.0093	0.022
	II	1.658	0.0526	0.139	-0.041	0.038	49.76	-0.0094	0.023
	III	2.223	0.0137	0.049	-0.011	0.012	15.23	-0.0045	0.086
	IV	2.073	0.0209	0.063	-0.017	0.016	21.14	-0.0050	0.087
High pressure phase (β' -glycine)									
0.9	I	1.765	0.0393	0.114	-0.030	0.029	38.07	-0.009	0.020
	II	1.662	0.0523	0.138	-0.041	0.038	49.36	-0.009	0.025
	III	2.052	0.0198	0.067	-0.016	0.017	21.66	-0.006	0.045
	IV	2.167	0.0172	0.058	-0.014	0.014	18.38	-0.005	0.136
	II'	<i>Critical point not found!</i>							
1.7	I	1.755	0.0403	0.117	-0.031	0.030	39.25	-0.009	0.022
	II	1.664	0.0521	0.138	-0.041	0.038	49.49	-0.009	0.026
	III	2.095	0.0182	0.065	-0.015	0.016	20.74	-0.006	0.059
	IV	2.095	0.0198	0.063	-0.016	0.016	20.61	-0.005	0.104
	II'	<i>Critical point not found!</i>							

Symmetry codes of acceptors in H-bonds: -x, y+1/2, -z, (II) x, y, z-1, (III) -x, y+1/2, -z, (IV) -x, y+1/2, -z+1)

Table S4 Comparison of selected calculated and experimental bond interatomic distances in the hydrogen bonds in β and β' glycine*

r, Å	O1...N (IV)		O2...N (bond III)		O1...H5 (bond IV)		O2...H5 (bond III)	
P, GPa	Tumanov <i>et al.</i> , 2008	This work	Tumanov <i>et al.</i> , 2008	This work	Tumanov <i>et al.</i> , 2008	This work	Tumanov <i>et al.</i> , 2008	This work
0.0001	3.078(20)	2.933	3.119(20)	3.050	-	2.233	-	2.118
0.9	2,997(25)	2.896	3.074(25)	2.895	-	2.167	-	2.052
1.7	2.996(25)	2.873	3.043(25)	2.897	-	2.095	-	2.095

* Numeration of atoms and hydrogen bonds as in Figure 1. Symmetry codes of acceptors in H-bonds: (III) -x, y+1/2, -z, (IV) -x, y+1/2, -z+1.

Table S5 Calculated elasticity moduli according to Voight, Reuss and Hill, as well as the anisotropy index of the linear compressibility of glycine at various external hydrostatic pressures.

P, GPa	K(Voight), GPa	K(Reuss), GPa	K(Hill), GPa	H _{min} , TPa ⁻¹	H _{max} , TPa ⁻¹	Hydrostatical compressibility anisotropy
0	29.95	21.66	25.80	-0.155	27.27	∞
0.2	30.95	22.45	26.70	-0.275	25.92	∞
0.4	31.92	23.39	27.65	-0.178	24.52	∞
0.7	33.46	24.82	29.14	-0.151	22.61	∞
0.9	30.92	21.42	26.17	-0.282	31.32	∞
1.7	35.99	26.29	31.14	0.399	26.70	66.979

The anisotropy of the elastic modulus is equal to the ratio of its maximum eigenvalue to the minimum one. In the case of negative compressibility, it is considered "infinite", which should be understood as the maximum possible non-equivalence of properties in different directions (Gaillac *et al.*, 2016).

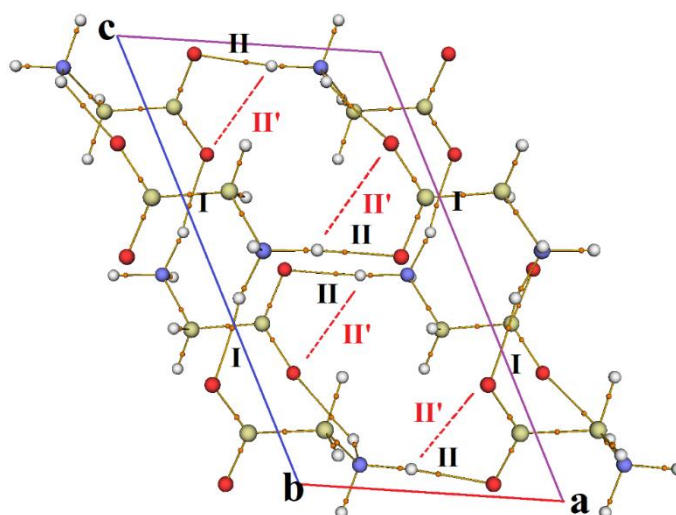


Figure S1 Molecular graph for a fragment of β' -glycine crystal structure. Poincare-Hopf condition ($0 = n - b + r - c$) if satisfied: $0 = 40 - 40 + 0 - 0$. Orange dots correspond to the bond critical points (BCP), yellow lines represent the bond paths. Red dotted lines are putative II' bond paths (were not confirmed by topological analysis of the electron density)

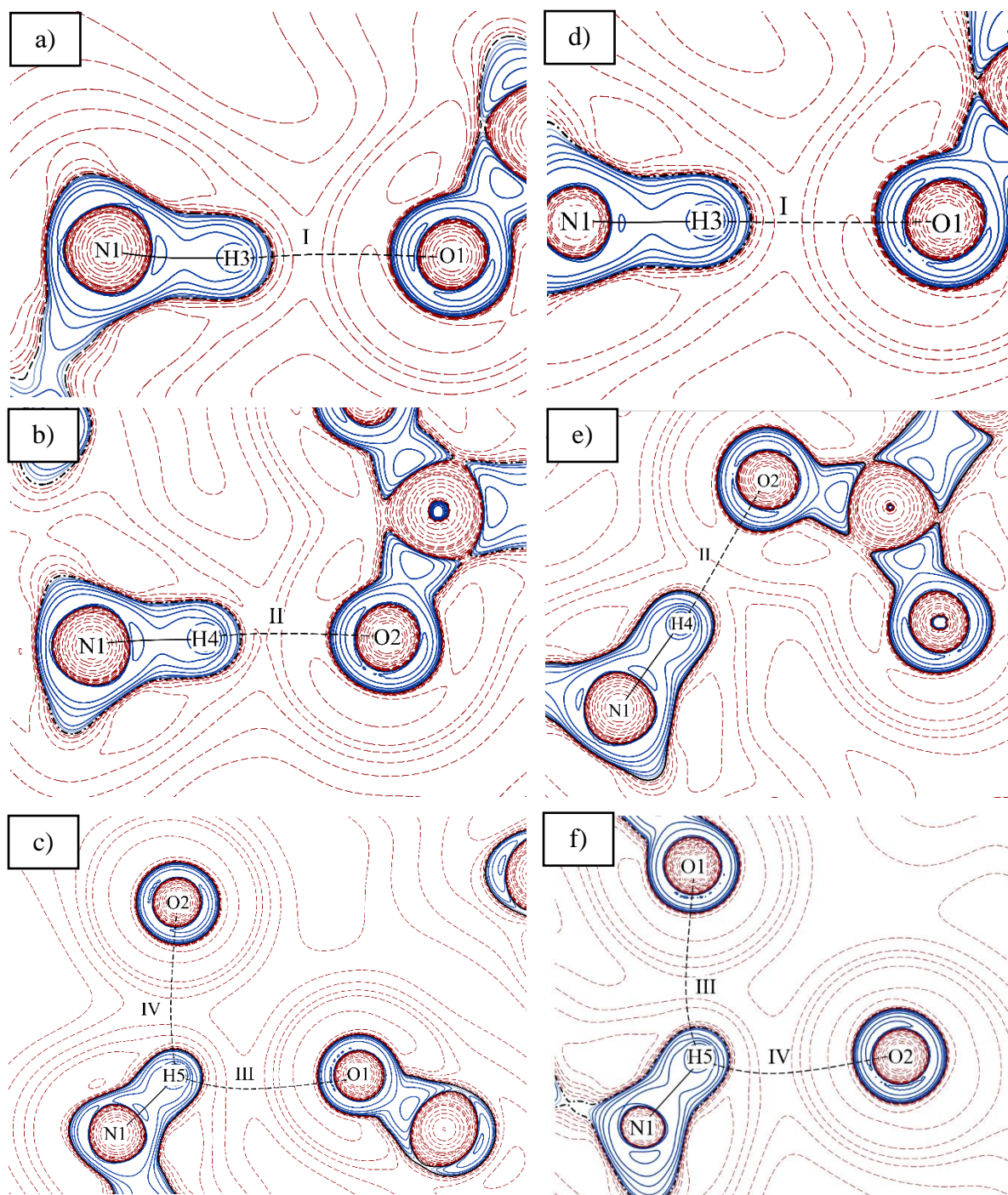


Figure S2 2D map of the electron density Laplacian in the planes corresponding to H-bonds at 0.0001 GPa (a, b, c) and a pressure above the phase transition point (0.9 GPa, d, e, f) Blue lines correspond to electron density concentrations. Isoline intervals are $\pm (2, 4, 8) \cdot 10^n$ a.u. ($-3 \leq n \leq 3$). Symmetry codes of acceptors in H-bonds: (I) $-x, y+1/2, -z$, (II) $x, y, z-1$, (III) $-x, y+1/2, -z$, (IV) $-x, y+1/2, -z+1$)

Comparison with data reported by Guerin, Stapleton et al. (2018)

Because of a significant discrepancy of our results with those reported earlier by Guerin (Guerin *et al.*, 2018), we attempted to reproduce the results calculated by Guerin *et al.*, (2018) which were based on the Iitaka (1960) structural data. The same PBE exchange functional and the plane-wave basis set were applied. As a result, under the same conditions, we obtained the value of $d_{16} = 65$ pm/V (Table 4). Guerin *et al.*, (2018) used the Density Functional Perturbation Theory (DFPT) (Wu *et al.*, 2005), in order to evaluate piezoelectric tensors. The DFPT and Berry-phase schemes give quite similar results when using the same shrinking factors (Baima *et al.*, 2016).

We can speculate about the reasons of this discrepancy. First, the PBE exchange functional is hardly suitable to describe elastic properties (Erba *et al.*, 2013). Second, the plane-wave basis set performs improperly for molecular crystals. And the last, but not the least, there is a difference in the XRD structural data for calculation inputs. Additionally, due to significant difference in C_{44} component of elastic tensor, as long as piezoelectric coefficients are proportional to elastic ones, it is not surprising that our shear constants (namely d_{16} , d_{14} , d_{25} , d_{34} , and d_{36}) do not match. Because of all these reasons, we think that our results are closer to the true values, than those of Guerin *et al.*, (2018). As for the experimental data, unfortunately, up to now, the only experimental data available, are those reported by Guerin. We would like to avoid any speculation on this issue. Instead, we appeal to experimentalists to further study this point.

Table S6 Comparison of piezoelectric coefficients (pm/V) by Guerin et al., (2018) and our attempt to reproduce them.

	PBE0/6-31G(d,p) (Present work, XRD data from Tumanov <i>et al.</i> , 2008)	PBE PAW (Guerin <i>et al.</i> , 2018, XRD data from Iitaka, 1960)	PBE/6-31G(d,p) (calculated in this work using XRD data from Iitaka, 1960)	PBE0/6-31G(d,p) (calculated in this work using XRD data from Iitaka, 1960)
d_{21}	-2.1	1.8	1.7	1.9
d_{22}	4.9	-5.7	-0.6	-4.6
d_{23}	-1.2	1.9	0.7	1.6
d_{14}	20.5	15.8	-22.2	-15.0
d_{16}	-15.1	195	65	46.7
d_{25}	0.78	5.1	-0.6	-0.4
d_{34}	-29.6	1.3	-0.3	0.3
d_{36}	28.5	7.5	-8.5	-8.9

Table S7 Cell parameters obtained from calculations using (Iitaka, 1960) XRD data with different basis sets

	a, Å	b, Å	c, Å	β , °	Volume, Å ³
XRD					
(Iitaka, 1960)	5.08	6.27	5.38	113.12	157
PBE0 6-31G(d,p)					
(Present work)	5.07	6.17	5.38	111.86	156
PBE 6-31G(d,p)					
(Present work)	5.11	6.22	5.43	111.56	160
PBE PAW without D3					
(Guerin, <i>et al.</i> , 2018)	5.13	6.39	4.99	112	164